STRANGENESS ENHANCEMENT IN SMALL COLLISION SYSTEMS AT ALICE: ROLE OF HARD AND SOFT PROCESSES*

Ishaan Ahuja

for the ALICE Collaboration

Faculty of Science, P.J. Šafárik University
Košice, Slovak Republic

Received 28 March 2025, accepted 9 October 2025,
published online 19 December 2025

Recent measurements in high-multiplicity proton–proton (pp) and proton–lead (p–Pb) collisions have exhibited features reminiscent of those observed in lead–lead (Pb–Pb) collisions. Among them, the observed enhancement of strange particle production as a function of multiplicity remains poorly understood. In order to probe the underlying mechanisms behind this phenomenon, we differentiate between strange hadrons originating from jets and those arising from soft processes. This is attained by using angular correlations between high transverse momentum charged particles and strange hadrons for K^0_S, Ξ, and ϕ in pp collisions at $\sqrt{s} = 13$ TeV and p–Pb collisions at $\sqrt{s_{NN}} = 5.02$ TeV. We observe that strangeness enhancement in small collision systems grows smoothly with charged-particle multiplicity and is predominantly driven by soft processes, while hard processes' contributions remain comparatively small.

DOI:10.5506/APhysPolBSupp.18.6-A13

1. Introduction

Strangeness enhancement was among the earliest proposed signatures for the formation of quark–gluon plasma (QGP), a state of matter with deconfined quarks and gluons governed by quantum chromodynamics [1]. In ultra-relativistic heavy-ion collisions that reach temperatures and energy densities conducive to QGP formation, strange hadron production increases relative to smaller collision systems (pp or p–Pb) [2], with multistrange baryons showing more pronounced yield enhancement compared to non-strange hadrons. Surprisingly, this enhancement can also be seen in smaller systems such as

* Presented at the V4-HEP 1 — Theory and Experiment in High Energy Physics Workshop, Bratislava, Slovakia, 26–28 July, 2023.

pp or p–Pb collisions as an increasing ratio of strange hadron to pion yields with growing charged-particle multiplicity. The ALICE measurements at the LHC revealed the smooth evolution of this ratio across various collision systems and energies, with enhancement magnitude scaling according to the particle's strangeness content [3].

2. Strange hadron detection with ALICE

ALICE identifies weakly-decaying strange hadrons in the central rapidity region via topological reconstruction of their charged decay products: $\Lambda \to p\,\pi^-$, $K^0_S \to \pi^+\pi^-$, and $\Xi^- \to \Lambda\,\pi^- \to p\,\pi^-\pi^-$ (and their charge conjugates). Kinematic and geometric selection criteria applied to reconstructed decay particles ensure that daughter tracks follow the expected decay topologies with a reduced combinatorial background. The invariant-mass technique is then used to identify the strange hadrons. For relatively short-lived resonances $\phi \to K^+ K^-$, where topological selections are not required, signal extraction can be performed by the invariant-mass technique solely.

3. Strange hadron production in hard and soft processes

In hadronic collisions, particle production occurs via hard (high momentum transfer) or soft (low momentum transfer) processes. Hard processes produce collimated hadron sprays called jets with the highest p_{T} charged hadron selected as the trigger particle, marking the jet axis and near-side region. Soft processes are governed by medium bulk properties, studied in out-of-jet regions. The ALICE results presented here use two-particle angular correlations to study strange hadron production in hard *versus* soft processes.

The two-particle angular correlation method [4] involves selecting the trigger particle and identifying strange hadrons in the $(\Delta\varphi,\ \Delta\eta)$ plane. A $p_{\mathrm{T}} > 3$ GeV/c selection is applied for trigger particles (unidentified charged hadrons). Associated particles (identified strange hadrons of interest with lower p_{T} than trigger) are correlated with the trigger particle using angular differences $(\Delta\varphi,\ \Delta\eta)$. The resulting distribution is categorized into towards leading (near-side jet), transverse-to-leading (out-of-jet/underlying event), and fully inclusive regions. Per-trigger yields of associated particles are computed and corrected for reconstruction efficiencies, detector acceptance, and non-primary particle contamination.

4. Results

We present h–K^0_S and h–Ξ correlations from minimum bias pp collisions ($\sqrt{s} = 5.02$ TeV), with their p_T spectra in figure 1. Near-side jet spectra are harder than out-of-jet spectra, reflecting distinct production mechanisms with the former dominated by hard processes. Full spectra closely follow out-of-jet spectra shapes, indicating their predominant contribution. K^0_S and Ξ per-trigger yields (Fig. 2) show stronger multiplicity dependence in transverse-to-leading and full regions compared to the near-side jet region, indicating a relatively higher contribution from soft processes with increasing multiplicity. The Ξ/K^0_S integrated yield ratio (Fig. 3) increases with multiplicity, reflecting Ξs higher strangeness content ($|S| = 2$) compared to K^0_S ($|S| = 1$). Out-of-jet and near-side jet ratios show compatible rises, and the near-side ratio magnitude suggests a smaller contribution to yield. No center-of-mass energy dependence is observed.

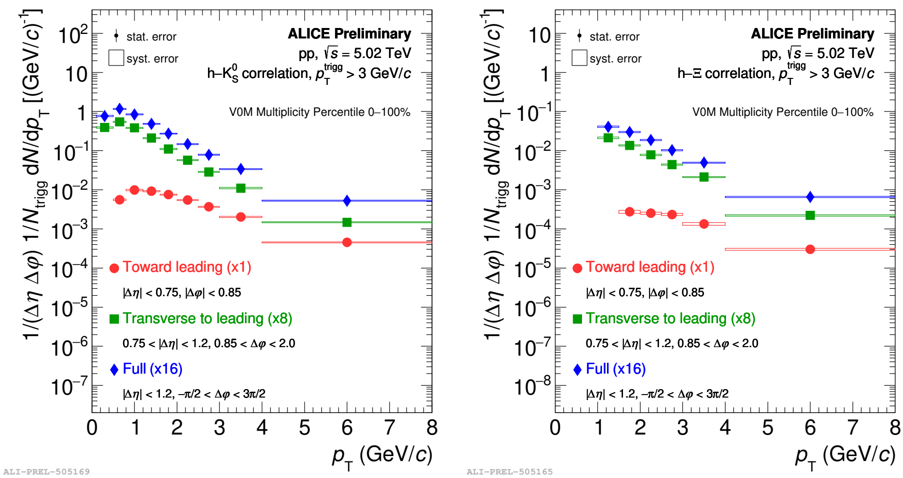

Fig. 1. Towards leading, transverse-to-leading, and full transverse momentum (p_T) spectra of K^0_S (left), Ξ (right) for pp collisions at $\sqrt{s} = 5.02$ TeV. Error bars represent statistical and empty boxes total systematic uncertainties.

Similar results are observed for h–K^0_S and h–Ξ correlations in high-multiplicity pp collisions ($\sqrt{s} = 13$ TeV) [5], h–Λ and h–ϕ correlations in p–Pb collisions ($\sqrt{s_{NN}} = 5.02$ TeV) [6, 7].

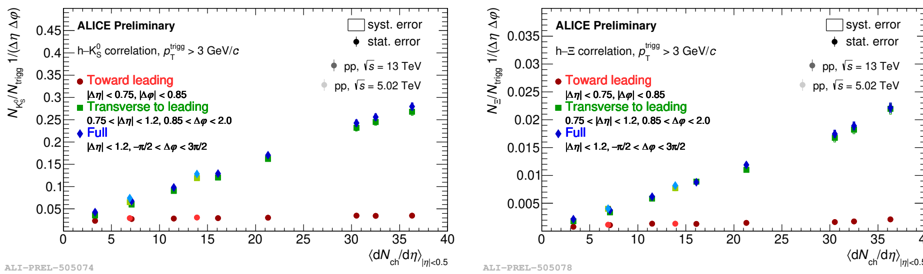

Fig. 2. K^0_S (left) and $\varXi$ (right) yields (integrated over full $p_{\mathrm{T,assoc}}$) per-trigger particle and per unit $\Delta\varphi\Delta\eta$ as a function of $\langle \mathrm{d}N_{\mathrm{ch}}/\mathrm{d}\eta\rangle_{|\eta|<0.5}$. Error bars represent statistical and empty boxes total systematic uncertainties.

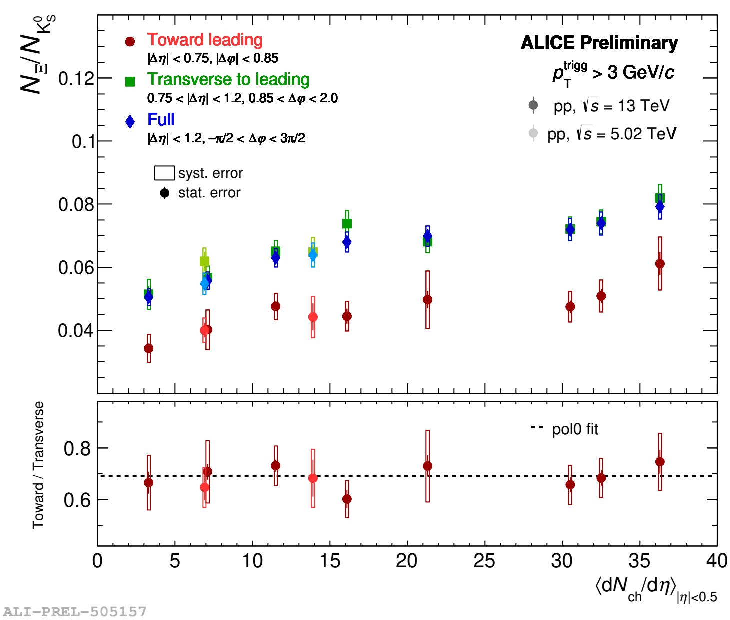

Fig. 3. $\varXi/K^0_S$ yield ratio (integrated over full $p_{\mathrm{T,assoc}}$) as a function of $\langle \mathrm{d}N_{\mathrm{ch}}/\mathrm{d}\eta\rangle_{|\eta|<0.5}$. Error bars represent statistical and empty boxes total systematic uncertainties.

5. Conclusions

Strange hadron production reveals a smooth trend correlating with multiplicity across various collision systems at different energies, with two-particle angular correlation studies showing distinct production mechanisms for strange hadrons in hard and soft processes, evidenced by harder p_{T} spectra for in-jet particles. Per-trigger yield ratios exhibit compatible multiplicity-dependent enhancement in both in-jet and out-of-jet regions, though the consistently larger contribution from out-of-jet regions indicates soft processes dominate strange particle production over hard scattering.

REFERENCES

[1] J. Rafelski, B. Müller, *Phys. Rev. Lett.* **48**, 1066 (1982).

[2] ALICE Collaboration (B.B. Abelev *et al.*), *Phys. Lett. B* **728**, 216 (2014), *Corrigendum ibid.* **734**, 409 (2014).

[3] ALICE Collaboration, *Nature Phys.* **13**, 535 (2017).

[4] ALICE Collaboration (B. Abelev *et al.*), *Phys. Lett. B* **719**, 29 (2013).

[5] ALICE Collaboration (S. Acharya *et al.*), *J. High Energy Phys.* **2024**, 204 (2024).

[6] ALICE Collaboration (S. Acharya *et al.*), *Phys. Rev. C* **110**, 064912 (2024).

[7] ALICE Collaboration (S. Acharya *et al.*), *Phys. Rev. C* **111**, 015201 (2025).